THE ASTROPHYSICAL JOURNAL, 288:175–181, 1985 January 1

THE FORM OF THE INITIAL MASS FUNCTION IN AN H II COMPLEX IN NGC 6946

KATHLEEN DEGIOIA-EASTWOOD
University of Wyoming
Received 1983 August 19; accepted 1984 July 20

ABSTRACT

Evidence is beginning to accumulate that the initial mass function (IMF) is not the same everywhere but suffers at least spatial variations. We have constructed a simple model aimed at determining the slope of the IMF in a cluster of young stars. We present narrow-band photometry of H II complex C in the Sc I galaxy NGC 6946 and compare the observations with the results of the model. The regions of the complex are very young and the observations fall in an ambiguous area of the model results; thus a precise value for the IMF slope is indeterminable. The star formation rate and efficiency of massive star formation are calculated using a Salpeter IMF and compared to the average values over the entire galaxy.

Subject index: galaxies: individual — nebulae: H II regions — stars: formation — stars: stellar statistics

I. INTRODUCTION

Knowing the mass spectrum of stars produced in each generation is crucial to theories of galactic evolution. In particular, the number of massive stars formed has a large influence on the rate and amount of metal production. In order to predict what form the initial mass function (IMF) takes, we need to identify those physical factors which influence that form. Measuring the form of the IMF and its variations are an important first step in identifying the influencing factors. In a previous work (DeGioia-Eastwood *et al.* 1984, hereafter Paper I) we measured the average Hα emission as a function of galactocentric radius in the late-type spiral galaxy NGC 6946. Assuming a Salpeter (1955) IMF, we calculated the star formation rate and star formation efficiency as a function of radius and considered the factors influencing those quantities. In this paper we present more detailed narrow band optical photometry of a giant H II complex in the same galaxy and, using a simple model, attempt to estimate the slope of the IMF in different regions of the complex.

The form of the IMF in the solar neighborhood was first deduced by Salpeter (1955) and approximated by a power law, that is

$$\frac{dN(m)}{dm} \propto \left(\frac{m}{m_\odot}\right)^{-2.35},$$

where $N(m)$ is the number of stars formed in the mass interval m to $m + dm$. This function has a slope which is constant in log m, although the range of validity as originally determined by Salpeter was only for log $(m/m_\odot)$ between -0.4 and $+1.0$. A more recent determination using a similar sample of stars by Miller and Scalo (1979) found the function to be well approximated by a half-Gaussian distribution in log m, a function which has a constantly changing slope in log m. However they also represented the function by a three-segment power law, each segment having a different slope. The function for $m \gtrsim 10$ $M_\odot$ is steeper than the Salpeter IMF, with an exponent of -3.3 instead of -2.35.

However, Garmany, Conti, and Chiosi (1982) have even more recently determined the slope of a power-law IMF for stars more massive than 20 $M_\odot$ from a catalog of galactic O type stars which is complete to a much larger distance than the samples of all spectral types used by Salpeter and by Miller and Scalo. They find a slope closer to Salpeter's, -2.6, for the entire sample, but also note a substantial difference in the slope between stars inside and outside the solar circle. Inside the solar circle the slope is close to Salpeter's; outside, the slope is close to Miller and Scalo's.

The findings of Garmany, Conti, and Chiosi (1982) are not the only evidence for a nonuniform IMF. Freeman (1977) found extreme variations among the slopes of the IMF for old globular clusters in our Galaxy and young globular clusters in the LMC. Scalo (1978) reviewed the rather ambiguous evidence for spatial and temporal variations in the IMF as well as in the value of the upper mass limit for individual stars. Since then, Jensen, Talbot, and Dufour (1981) have found indirect evidence for spatial variations in the IMF as well as variations from the mean solar neighborhood IMF as a function of position in M83.

Obviously it would be useful to be able to determine the IMF of a very young cluster from observations of the bulk properties of the region rather than by counting individual stars. In principle a comparison of the gaseous line emission, excited by the most massive stars, and the continuum emission, produced by all stars present, should yield some measure of the slope of the IMF. In this work we express this idea in a simple model and then attempt to determine the slope of the IMF in a giant H II complex in NGC 6946.

II. THE MODEL

The goal of the model is to be able to estimate the slope of the present-day epoch IMF for the stars being formed within an H II region using narrow-band photometry or spectrophotometry. In the model we compute the colors and hydrogen emission for a cluster of young stars. The results are distinct if the cluster is older than about 2×10^7 years or if the exponent in a power-law IMF is greater than about three. The model is intended to be used with observations of extragalactic H II regions where the emission of the underlying disk is known sufficiently accurately to be subtracted. With galactic H II regions extreme care must be taken to include a sufficiently large diffuse region in the observations, not simply the small cluster of massive stars at the center of an extended region. This should ensure that enough smaller stars are included so that the sample of observed stars is statistically complete.

The model is similar in concept to that of Shields and Tinsley (1976). In the model we numerically integrate the monochromatic continuum emission and hydrogen line emission for a cluster of coeval main-sequence stars in a cloud of hydrogen as a function of the age of the cluster and the slope of a power-law IMF. The output parameters are monochromatic colors and the ratios of Hβ line emission to monochromatic flux.

In our calculation all quantities were indexed by the stellar mass, where the range extended from $\log(m/m_\odot) = -1.0$ to 1.8 in steps of 0.1 dex. As discussed later, the choice of upper mass limit effectively specifies the youngest determinable age. The choice of lower mass limit strongly affects the total mass integrated along the IMF, but at the blue wavelengths and young ages considered here makes no effect on the output parameters.

In order to have a well-determined empirical relationship as the basis of the calculation, we used the mass-luminosity relation between the mass and M_v, the absolute Johnson broadband V magnitude (Allen 1973). We used data from both Allen and Panagia (1973) to interpolate for the effective temperature of main-sequence stars as a function of M_v. The stellar monochromatic continuum fluxes for each stellar type were then taken from the stellar atmosphere models of Kurucz (1979). The continuum wavelengths considered here are $\lambda\lambda$3560 and 4500, hereafter called u and b.

The blue supergiant phase of each star with a mass greater than about 6 $M_\odot$ was represented in the H-R diagram by a single point determined from the evolutionary tracks of Stothers and Chin (1977, 1979). For the most massive stars we chose their case B with the Schwarzschild convection criterion. The bolometric corrections to convert $L/L_\odot$ to M_v were taken from Allen (1973).

In the model we consider the blue supergiant phase of stars more massive than 6 $M_\odot$ but we do not consider the red supergiant phase. The contributions to the stellar flux by a reasonable number of M supergiants were found to contribute less than 1% of the total flux at the wavelengths shorter than λ4861 which are used here.

The flux of Lyman-continuum photons for each early-type star was taken from Panagia (1973) and converted to hydrogen line emission (Osterbrock 1974) and gaseous continuum emission by the free-bound, free-free, and two-photon processes (Brown and Mathews 1970). The nebula is assumed to be ionization bounded. Only solar abundances were considered. Further details of the model are given in DeGioia-Eastwood (1984), where the results for additional ultraviolet wavelengths are presented.

The results of the model are contained in Figure 1, where Hβ/b is plotted against u–b. The units of b are ergs s^{-1} cm^{-2} Å^{-1} and $u - b$ is defined as 2.5 log (b/u). Each locus of points represents a separate slope of a power-law IMF as in the equation above. The age of the cluster increases down each locus of points. The dsahed horizontal curves are lines of constant age. The slope is represented in the figure by β, where $\beta = 2.35$ is a Salpeter (1955) IMF. The Miller and Scalo (1979) IMF is included for comparison and labeled MS.

A large β, i.e., the IMF being steeper, means fewer early-type stars for the same number of late-type stars, and thus the continuum is redder and the relative number of Lyman-continuum photons is smaller. The paucity of ionizing photons results not only in less hydrogen line emission but in less gaseous continuum emission also, so the loci are stretched farther along the $u - b$ axis than would be expected from the main-sequence stellar continuum alone. The addition of blue supergiants, however, tends to redden the total continuum since the supergiants' large luminosities and A–F spectral types make large contributions redward of b. It is the presence of the blue supergiants which makes the slope of the IMF distinguishable only for cluster ages greater than or equal to 2×10^7 years or for values of β roughly greater than or equal to three. The loci are similarly convergent for ultraviolet wavelengths but the total spread in magnitudes becomes greater (DeGioia-Eastwood 1984).

It should be noted that for most of the values of β presented here the continuum fluxes are dominated by the upper end of the main sequence. For all $\beta \gtrsim 2.35$, the fluxes of u, b, and Lyman-continuum photons peak at the highest mass star present at each age considered. The greater β becomes, the flatter the distribution of continuum flux becomes as a function of stellar mass. When all masses of stars are represented, only for $\beta \gtrsim 3$ does one see lower than about 10 $M_\odot$, and only for $\beta \gtrsim 4$ does one see down to 1 $M_\odot$, even at b. This is not too unfortunate since it is unlikely that the IMF can be truly represented by a power law in most cases.

III. OBSERVATIONS

a) *The Data*

The observations presented here are of the giant H II complex labeled "C" by van der Kruit, Allen, and Rots (1977) in their radio continuum study of NGC 6946. The galactocentric distance of the complex is about 2'.5, or 7.2 kpc at a distance of 10 Mpc. We have broken up the complex into three regions: C1, C2, and C3. The coordinates and dimensions of the three regions are included in Table 1.

The data were obtained on the Wyoming 2.3 m telescope during 1982 June, July, and August. The instrument was a photoelectric photometer equipped with a Varian S-surface photomultiplier tube and a set of circular variable filters. The passband centers and FWHM bandwidths are given in Table 2, and will be referred to hereafter as u (λ3560), b (λ4500), Hβ, O III, r (λ6200), and Hα, although they are *not* standard Strömgren filters. Hα was included to determine the extinction by comparison with Hβ, and O III was included to give some indication of the metal abundance when compared with Hβ. The b and r filters served as measurements of the continuum for the emission lines after taking the slope of the continuum into account. For purposes of comparison with the model we converted the fluxes through the continuum filters to average monochromatic fluxes.

We used the WIRO fast-mapping telescope control routines (Hackwell, Grasdalen, and Gehrz 1982) to obtain digitized maps 64 arcsec on a side. The area was sampled every 2″, giving a 32 × 32 pixel frame. A 7″ beam was used in all the frames, and each individual frame had a total integration time of about 10 minutes. The total number of frames of each wavelength co-added to give each final image is included in Table 2. After each 10 minute frame the sky was monitored using spot photometry on several places found free of stars on the Palomar Observatory Sky Survey.

The random errors in the uncorrected fluxes for synthetic aperture photometry determined from the co-added frames range from 2% for r and Hα to 6% for O III. These errors are included in Table 2. Since the value for the flux in each emission line depends on the difference between two fluxes, the errors for the emission lines are slightly larger. These errors amount to 3% for Hα, 5% for Hβ, and 7% for O III.

TABLE 1

OBSERVED PARAMETERS OF H II COMPLEX

Region	C1	C2	C3
α_{1950}	$20^h34^m01^s.96$	$20^h34^m03^s.92$	$20^h34^m04^s.36$
δ_{1950}	60°00′29″.8	60°00′47″.1	60°00′23″.1
Diameter (arcsec)	20.7 (square)	17.3 (square)	16.7 (circular)
Hα/Hβ	9.86	5.89	4.97
A_v (mag)	3.67	2.13	1.64
O III/Hβ[a]	1.32	0.71	0.85
Hβ emission (ergs s^{-1} cm^{-2})	4.03×10^{-12}	6.10×10^{-13}	2.33×10^{-13}
$(u-b)$[a,b]	−0.42	−0.27	0.10
log $(H\beta/b)$[a,b]	1.49	1.67	1.48

[a] Corrected for extinction, cloud assumed at midplane.
[b] u and b are in units of ergs s^{-1} cm^{-2} Å^{-1}, and $u-b$ is 2.5 log (b/u). Also, these ratios are distance independent.

b) *Calibration Procedures*

Using the Wyoming image processing system we converted the raw data to a calibrated position-intensity matrix. The monochromatic air-mass corrections were interpolated from the data of Hayes (1970) and are included in Table 2. We then reduced the data to absolute fluxes using observations of Stone's (1977) standard stars and the recalibration of Vega by Hayes and Latham (1975). The values for each separate region of the H II complex were obtained by doing synthetic aperture photometry with the image processor.

c) *Calculation of the Extinction*

The extinction was computed by comparing the observed ratio of Hα/Hβ to the theoretical value of 2.87 given by Osterbrock (1974). All theoretical parameters in this work are taken for case B, where the nebula is optically thick in the Lyman lines, and for an electron temperature of 10,000 K. However, since the observed fluxes of Hα and Hβ depend slightly on the value chosen for the slope of the continuum emission, and since that slope itself depends upon the extinction, we solved for consistent values of the extinction and the straight line interpolated continuum slope using an iterative process.

The determination of the Hα flux is complicated by the presence of the [N II] lines at λλ6548 and 6583 within our bandpass. In Paper I we corrected the data using a relationship between [N II]/Hα and R/R_{25} (de Vaucouleurs, de Vaucouleurs, and Corwin 1976) derived from the data of Smith (1975) for giant H II regions in galaxies of similar morphological type. For the H II complex C we also had information on the "excitation," the O III/Hβ ratio. Relating the excitation to the [N II]/Hα ratio, we found that the [N II]/Hα ratio corresponding to the measured excitation was slightly greater than would be expected from the R/R_{25} of H II complex C. A multiplicative factor of 0.7 was applied to all the Hα emission to correct for the [N II] lines. Since the O III and Hβ lines are so close together in wavelength, their ratio is not much affected by any changes in the continuum slope; this analysis was performed independently of the iteration process.

TABLE 2

FILTERS AND UNCORRECTED FLUXES

Designation	u	b	Hβ	O III	r	Hα
Center λ(Å)	3560	4500	4861	5003	6200	6562
FWHM (Å)	138	141	73	78	133	157
Number of 10 minute frames	8	6	5	3	8	6
Air mass correction (mag airmass^{-1})	0.624	0.272	0.223	0.203	0.143	0.112
Uncorrected Flux (ergs s^{-1} cm^{-2} × 10^{13})						
C1	1.93	3.59	2.62	2.41	6.04	17.7
C2	1.40	1.16	1.73	1.57	9.11	3.18
C3	1.28	2.37	1.68	1.65	3.96	7.96
Surrounding Disk (ergs s^{-1} cm^{-2} arcsec^{-2} × 10^{16})						
Surrounding Dish	2.65	5.98	3.65	3.31	9.93	16.2
Error (percent)	5	3	4	6	2	2

The values of the excitation (O III/Hβ) in the three regions are 1.32, 0.71, and 0.85 (included in Table 1), with an average value of 0.96 or −0.02 in the log. Variability of the excitation within a single H II region was also found by Talent and Dufour (1979) in observations of local galactic H II regions. However, this average value of the excitation, while perfectly consistent with Smith's (1975) observations of H II regions in other late-type galaxies, is lower by about a factor of 2 than the average values found by Talent and Dufour.

Since in our Galaxy and in Smith's samples of Scd and Sbc galaxies there is a gradient in the excitation in the sense that the excitation increases with radius, the low excitation would indicate that H II complex C should be more similar to those inside the solar circle than out. Thus we expect higher heavy element abundances and a lower electron temperature than in the solar neighborhood, since it is the forbidden lines of O and N such as the λλ4959 and 5007 [O III] lines we consider here which provide the main cooling mechanism for H II regions. For these reasons we might expect the IMF to be less steep than in the solar neighborhood, consistent with Garmany, Conti, and Chiosi's (1982) result. Unfortunately the results we present here are too indeterminate to test this hypothesis.

The consideration of the extinction was further complicated by the fact that our model requires observations of just the H II complex and not the surrounding disk. If the H II complex is fairly opaque to the disk emission, then the subtraction of the disk component becomes model dependent. We considered three separate cases, where the complex is at the back, center, and front of the galactic disk with respect to the observer. Since

each region in the complex did turn out to be fairly opaque, this is roughly equivalent to subtracting all, half, or none of the disk.

The derived value of the extinction varied little from case to case for each of the three regions in the complex. However, since the complex is roughly equal in brightness to the disk, the amount of disk subtracted makes a substantial difference in the flux attributed to the complex, and the derived values of the colors of the complex changed considerably with the case considered. The derived values for the three cases are shown along with the model predictions in Figure 1. However, we consider the second case, where the complex lies on the midplane of the galactic disk, to be so much more likely than the other two that it is the only case we consider for the remainder of this paper.

Our model of the extinction assumes that most of the extinguishing dust lies outside the gaseous emitting region (see next paragraphs for justification). If we assume the emitting region to be at the center of a cloud and the Hα/Hβ ratio of the emission indicates an optical depth τ, then the total optical depth across the entire cloud is 2τ. For a cloud on the midplane of the galactic disk, this involves taking the intensity of the unextinguished disk, measured adjacent to the complex, into account in this way:

$$I_{\mathrm{H}\alpha_{\mathrm{obs}}} = \tfrac{1}{2} I_{\mathrm{disk}} + \tfrac{1}{2} e^{-2\tau} I_{\mathrm{disk}} + e^{-\tau} I_{\mathrm{H}\alpha} .$$

It is the A_v corresponding to the τ in this equation that we include in Table 1.

We would like to note that the high values of Hα/Hβ (see Table 1) indicate that a large part of the dust is outside the ionized region. Mathis (1970) notes that "unblanketed" models (where all the dust is inside the emitting region of the nebula) approach finite values of Hα/Hβ in the limit of infinite optical depth. Our simple solution to the transfer equation for our models indicate that Hα/Hβ would have a maximum value of 3.87 if all the dust were coincident with the emitting gas. Since our values of Hα/Hβ exceed this value, we have assumed that the extinguishing dust is external to the emitting region in our models of the extinction.

It is possible to check this assumption using the volumes and electron densities derived below in § IV. Assuming that $n_e \approx n_{\mathrm{H}}$ and that one-half the thickness of the cloud is about 50 pc, we take the value of $\langle N(\mathrm{H\ I} + \mathrm{H}_2)/E(B-V)\rangle = 5.8 \times 10^{21}$ atoms $\mathrm{cm}^{-2}\ \mathrm{mag}^{-1}$ derived by Bohlin, Savage, and Drake (1978) and calculate the A_v expected from the number of atoms which fit into the volume of the cloud. This calculation produces A_v values of 1.1, 0.47, and 0.31 for regions C1, C2, and C3; these are a factor of 5 less than the values of A_v calculated from the observed Hα/Hβ ratio. We consider this additional evidence that most of the extinguishing dust is outside the emitting regions of the nebulae.

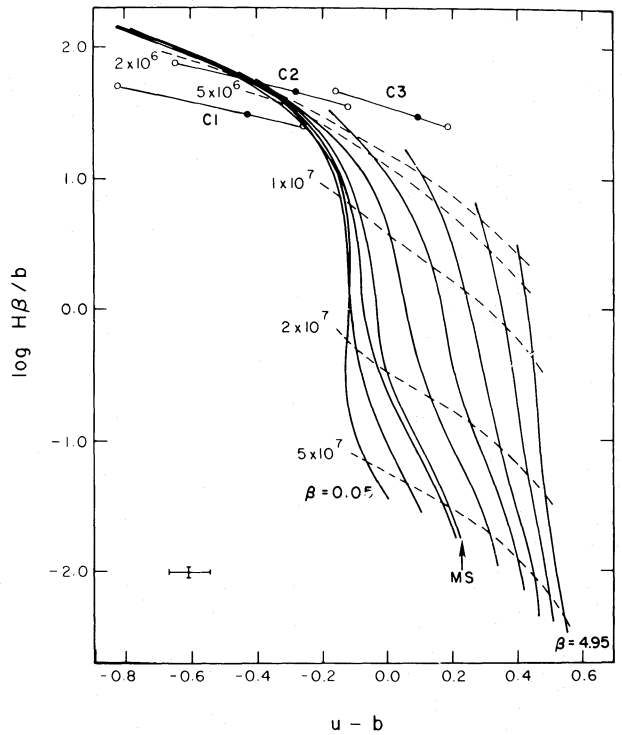

FIG. 1.—The logarithm of Hβ/b plotted against $u - b$. Each vertical locus of points represents a separate β, where β is the slope of a power-law IMF as noted in the text. A Salpeter IMF corresponds to $\beta = 2.35$. The results for a Miller and Scalo IMF are labeled as MS. From left to right, the values of β represented are 0.05, 1.35, 2.35, Miller and Scalo, 3.35, 3.85, 4.25, 4.65, and 4.95. The horizontal dashed curves are lines of constant age, with the age for each line marked in years. The data for H II complex C have been plotted on the graph for comparison. The central solid dots correspond to the results for each region for the case where the complex is assumed to be at the midplane of the galactic disk. The leftmost and rightmost circles, connected through each solid dot by a straight line, represent the result for the complex assumed in back and in front of the disk respectively. The three sets of points, from left to right, represent regions C1, C2, and C3 as designated in the text. The photometric error bars are shown in the lower left corner.

d) Comparison with Radio Continuum Observations

Van der Kruit, Allen, and Rots (1977) have tabulated the 6 cm and 21.2 cm fluxes of several giant H II complexes in NGC 6946. Their corresponding optical diameter for H II–C, however, listed in their Table 6, would seem to indicate that they have considered only our region C1, which is by far the brightest of the three regions we consider. Calculating the expected free-free flux at 21.2 cm from our extinction-corrected hydrogen emission lines, we find that we estimate about half again as much flux at 21.2 cm as they attribute to thermal flux. However, if we recalculate the extinction using the ratio of 21.2 cm flux to Hβ flux, we find that the result in the $u - b$ versus Hβ/b plane changes only very slightly.

IV. COMPARISON BETWEEN THEORY AND OBSERVATIONS

a) Regions C1 and C2

The two brightest regions of the three are C1 and C2. C1 also appears the largest on optical photographs and seems to be the region referred to by van der Kruit, Allen, and Rots (1977). Both regions lie near each other in the Hβ/b versus $u - b$ plane of Figure 1. Unfortunately, both regions lie very close to the convergence of loci in the very young area of the model output. Both appear to have ages of less than 10^7 years. Given the close convergence of the loci near the data points and the errors inherent in any model, however, it seems imprudent to assign values for the slope of the IMF.

Since we consider no variations in metallicity and have measured no other spectral lines besides Hα, Hβ, and O III, our model cannot distinguish between the effects of aging in a cluster and variations in the intrinsic upper mass limit (cf. Shields and Tinsley 1976). For example, a cluster of age 6×10^6 years which formed stars of up to 60 $M_\odot$ appears the

same as a much younger cluster which has simply not formed any stars more massive than 25 $M_\odot$. For this reason our determined ages are to be considered upper limits.

b) Region C3

By far the faintest region of the three considered is C3. Its placement in the Hβ/b versus $u - b$ plane suggests that the slope of its IMF is much steeper than the other two regions, as steep as $\beta = 4.45$, with an age of perhaps 10^6 years. The faintness of the region, however, indicates that there are not many early-type stars present. After completing the analysis presented below, we feel that the colors of the region may have been affected by small number statistics and that actually the region is more likely to have an IMF slope similar to that of the other two regions measured.

Given a form, slope, and upper mass limit for the IMF and an actual intensity of a hydrogen line, it is easy to calculate the number of stars present of each mass. This is done by adding up the number of Lyman continuum photons from each star and comparing the total with the intensity of the hydrogen line. We have done this for region C3, assuming a distance to NGC 6946 of 10 Mpc (see § V for a discussion of the distance).

We estimate that region C3 contains only 20.6 stars between 50 and 60 $M_\odot$ if we assume an IMF with a slope of 4.45. Since the numbers are small enough to expect the distribution of stars in region C3 to be Poissonian, the standard deviation of the number of stars present of a given mass will be equal to the square root of that number. Thus between 50 and 60 $M_\odot$ we expect 20.6 ± 4.5 stars, and between 40 and 49.9 $M_\odot$ we expect 51.0 ± 7.1 stars.

Next we consider the number of stars present in C3 computed using the same data but a slope of 3.45, a more moderate slope which is still considerably steeper than a Salpeter. A young region with this slope would fall in the convergent region of the model results. For this slope we have 26.9 ± 5.2 stars between 50 and 60 $M_\odot$, and 54.0 ± 7.3 stars between 40 and 49.9 $M_\odot$. Thus the plus or minus one standard deviation numbers overlap for the two slopes. This is also true for the third bin, 30–39.9 $M_\odot$. Thus observationally it is difficult to pin down the real slope for a faint region. Therefore we do not feel that we have proved the existence of a much steeper slope for this region.

Another interesting aspect of this calculation is the huge number of stars predicted at the lower masses. Even with a lower mass cutoff of only 0.1 $M_\odot$, the total masses predicted by our model from the observations are on the order of 10^{10} $M_\odot$. This unphysical result is not obtained from a Salpeter when a cutoff of 0.1 $M_\odot$ is used. Thus it seems unwise to extrapolate the data, which is dominated by the light of early-type stars, to the lower portion of the main sequence. This result also indicates that a straight power-law IMF is not suitable when very different from a Salpeter IMF.

V. CALCULATED PARAMETERS OF THE H II REGIONS

a) The Electron Density

The first physical parameter of the regions we attempted to calculate was the electron density, N_e. This calculation requires several assumptions. The first concerns the shape of the emitting volume. Since NGC 6946 is nearly face on, and since the individual regions are nearly a kiloparsec across, we assume a short cylindrical volume—a "pancake"—instead of a spherical one. We consider the existence of a spherical cloud that large unlikely and expect an association of smaller clouds within the cylindrical volume. We further assume the "pancakes" to have depths of 100 pc in the line of sight as a typical thickness of a giant molecular cloud complex (Cohen and Thaddeus 1977; Blitz and Thaddeus 1980). Since the effective filling factor is unknown we consider these to be maximum volumes. The diameters and volumes are included in Table 3.

TABLE 3

CALCULATED PARAMETERS OF H II COMPLEX

Region	C1	C2	C3
N_{Lyc} (photons s^{-1})	1.0×10^{53}	1.5×10^{52}	5.7×10^{51}
Diameter (pc)	1000	840	810
Volume (cm^3)	2.3×10^{63}	1.6×10^{63}	1.5×10^{63}
N_e (cm^{-3})	13	5.8	3.8
SFR[a] (Salpeter) ($M_\odot$ Gyr^{-1})	7.0×10^{8}	1.0×10^{8}	3.9×10^{7}
SFR[a] (Salpeter) ($M_\odot$ Gyr^{-1} pc^{-2})	7.0×10^{2}	1.4×10^{2}	6.0×10^{1}
Cloud mass ($M_\odot$)	8.7×10^{7}	3.6×10^{7}	2.5×10^{7}
SFE[b]	4.9×10^{-3}	1.8×10^{-3}	9.4×10^{-4}

[a] Mass range 0.1–60 $M_\odot$.
[b] Mass range 10–60 $M_\odot$.

The linear diameters of the regions are dependent on the assumed distance to the galaxy. Throughout this work we have assumed a distance of 10 Mpc (Sandage and Tammann 1974). Other estimates of the distance have been 5 Mpc by de Vaucouleurs (1979) and 7 Mpc by Israel (1980). Thus we consider the error in the distance to be a factor of 2 at the most. We consider the value of 100 pc for a typical molecular cloud complex good to about a factor of 3, thus making the volume estimates good only to about an order of magnitude.

The second assumption needed is that the nebula is ionization bounded and that the volume considered is the volume of the Strömgren (1937) sphere. Israel, Goss, and Allen (1975) found evidence in M101 that the giant H II complexes are generally ionization bounded. Then the condition

$$N_{Lyc} = V N_e^2 \alpha_B$$

will hold for case B in a pure hydrogen nebula (Osterbrock 1974), where N_{Lyc} is the number of Lyman continuum photons per second present, V is the volume of the Strömgren sphere, N_e is the number density of electrons ($N_e = N_p = N_H$ in a pure hydrogen nebula), and α_B is the effective recombination coefficient for case B.

Since we have measured N_{Lyc} through the hydrogen emission lines and have calculated a maximum volume, we can solve for a minimum electron number density. The resulting values range from 4 to 13 cm^{-3} for the three regions and are included in Table 3, along with the values of N_{Lyc}.

Our values for N_{Lyc} depend on the Hα photometry, for which we calculate a 1 σ standard deviation of about 10%. This estimate includes the uncertainty in the placement of the complexes relative to the galactic midplane. The absolute values also depend on the square of the distance to the galaxy, good to a factor of 4 as previously discussed. However, the distance dependence of N_{Lyc} and the volume cancels out in the calculation of N_e, leaving N_e dependent only on Hα and the square root of the assumed cloud depth. Thus the values of N_e are good to about a factor of 2.

The sizes and densities of these regions assure that they could be included with the sample of H II regions considered by

Smith (1957), which are large ($d \gtrsim 50$ pc) and of low density ($N_e \lesssim 500$ cm^{-3}). These are dissimilar to the more familiar nearby H II regions such as the Orion Nebula, which is much smaller and denser.

b) *The Star Formation Rate*

The second parameter of interest is the current star formation rate (SFR). Since the data are dominated by the light from the most massive stars, it would be preferable to use only the mass of these stars in our calculations. However, for purposes of comparison with the literature, we used a standard Salpeter IMF with mass limits of 60 $M_\odot$ and 0.1 $M_\odot$ to calculate the SFR.

As in Paper I, we used the mass in newly formed stars implied by the number of Lyman-continuum photons present and the given IMF. We then divided by the average age of an H II region, for which we chose the main-sequence lifetime of a 25 $M_\odot$ star, 6×10^6 years. We feel that it is appropriate to use this average age no matter what the actual age of the H II region is. Again as in Paper I we also present the SFR per square parsec, which is a quantity independent of distance. The calculated values of the SFR are shown in Table 3.

Both versions of the SFR depend on the Hα photometry and on the derived conversion rate between Hα photons and solar masses per year. This "conversion rate" in turn depends on assumptions such as shape and cutoff of the IMF and the chosen average star-forming time. Comparison of our conversion rate with other authors (Mezger 1978; Jensen, Talbot, and Dufour 1981; Hunter, Gallagher, and Rautenkranz 1982) indicates a spread of about an order of magnitude. This spread must be taken into account when interested in absolute rather than relative rates and when comparing our results with those of other authors. The SFR expressed as $M_\odot$ is also subject to an additional uncertainty of a factor of 4 due to the distance dependence.

The highest derived value of the SFR, $7.0 \times 10^2\ M_\odot\ \mathrm{Gyr}^{-1}\ \mathrm{pc}^{-2}$, is about 4 times as high as the highest values of the average SFR as a function of radius measured for NGC 6946 (Paper I). Since the assumptions made in Paper I are identical to those made here, this comparison is good to the accuracy of the photometry, about 10%.

This value is also about twice as high as the highest average SFR in M83, taking into account the factor of two difference in the conversion rate of Jensen, Talbot, and Dufour (1981). The largest value for the average SFR of irregular galaxies in the study by Hunter, Gallagher, and Rautenkranz (1982) was about 1000 $M_\odot\ \mathrm{Gyr}^{-1}\ \mathrm{pc}^{-2}$. The inferred conversion rate is roughly a factor of six higher than ours. Allowing for this difference, our value of 7.0×10^2 is again about 4 times as high as their largest value. It is not surprising that the local SFR for this single H II complex, one of the most active star forming regions in NGC 6946, is higher than the value of the SFR averaged over arm and interarm, active and inactive regions in different galaxies.

c) *The Efficiency of Massive Star Formation*

Although no detailed CO data are available to infer the gas mass so that the local star formation efficiency (SFE) can be calculated directly, we can estimate the mass of the cloud from the amount of extinction present. Since we have already shown (§ III) that most of the dust present is outside the emitting region, if we assume that the gas-to-dust ratio is the same in NGC 6946 as in our Galaxy, we can use the average relationship between column density and magnitudes of extinction to calculate the number of atoms which are causing the extinction.

Bohlin, Savage, and Drake (1978) found $\langle N(\mathrm{H\ I} + \mathrm{H}_2)/E(B-V)\rangle = 5.8 \times 10^{21}$ atoms cm^{-2} mag^{-1}, where $N(\mathrm{H\ I} + \mathrm{H}_2) = N(\mathrm{H\ I}) + 2N(\mathrm{H}_2)$. Applying this conversion factor to our measured values of A_V and using $R = A_V/E(B-V) = 3.08$, we find gas masses on the order of $10^7\ M_\odot$. Since our A_v only refers to the extinction between the observer and the center of the cloud, we further multiply these masses by 2. These final cloud masses are included in Table 3.

In reality the masses derived in this manner do not refer strictly to the single cloud in question but to the sum of all the clouds along the line of sight. Since gas surface densities are usually the only data available, and since the observed star formation is also necessarily integrated along the line of sight, it is customary to use this integrated mass in the efficiency calculation (cf. Talbot 1980). This is not strictly correct, but we present the calculation for purposes of comparison.

Given the cloud masses, the SFE is then simply the mass in newly formed stars divided by the mass of the cloud. Since the data are dominated by the massive stars, as in Paper I we use only the more massive stars. Using the masses down to 10 $M_\odot$ implied by the Salpeter IMF, we calculated the SFE for massive stars for each region and found it to be on the order of 10^{-3}. The values are included in Table 3.

The masses for the stellar content are subject to almost all of the errors previously discussed—photometry, model assumptions, distance. Taking all these errors into consideration, we do not expect the absolute values of the SFE to represent the real SFE inside a single cloud to more than about two orders of magnitude. However, when comparing the values of the SFE to the average values derived in Paper I, the assumptions and distance all cancel out, and we expect the comparisons to be good to better than a factor of 2.

The efficiencies calculated for H II complex C are about an order of magnitude higher than those found using the average Hα emission over the disk and cloud masses inferred from average CO emission in Paper I. Once more this is not surprising since H II complex C is one of the most intensely active star-forming spots in NGC 6946.

In summary, we have tried to estimate the slope of the IMF and the ages of three regions of a giant H II complex in NGC 6946 using a simple model of a cluster of stars in a hydrogen cloud. The results of our model are only distinct for a cluster older than about 2×10^7 years or if the IMF is steeper than a Salpeter IMF. Our observed regions are very young and unfortunately fall close to an ambiguous area of the model output, so we do not feel that we have pinned down the IMF slopes. We find that the SFR and SFE for a single region calculated with a Salpeter IMF (for purposes of comparison) predict a SFR about 4 times higher than the highest average value for the entire galaxy, and a SFE an order of magnitude higher than the average value over the same area.

The author thanks Steve Strom and Gary Grasdalen for their help and the referee, Glenn Miller, for his useful comments. This work was supported by the National Science Foundation.

REFERENCES

Allen, C. W. 1973, *Astrophysical Quantities* (3rd ed.; London: The Athlone Press).
Blitz, L., and Thaddeus, P. 1980, *Ap. J.*, **241**, 676.
Bohlin, R. C., Savage, B. D., and Drake, J. F. 1978, *Ap. J.*, **224**, 132.
Brown, R. L., and Mathews, W. G. 1970, *Ap. J.*, **160**, 939.
Cohen, R. S., and Thaddeus, P. 1977, *Ap. J. Letters*, **217**, L155.
DeGioia-Eastwood, K. 1984, *Pub. A.S.P.*, **96**, 625.
DeGioia-Eastwood, K., Grasdalen, G. L., Strom, S. E., and Strom, K. M. 1984, *Ap. J.*, **278**, 564 (Paper I).
de Vaucouleurs, G. 1979, *Ap. J.*, **227**, 380.
de Vaucouleurs, G., de Vaucouleurs, A., and Corwin, H. C. 1976, *Second Reference Catalog of Bright Galaxies* (Austin: University of Texas).
Freeman, K. C. 1977, in *The Evolution of Galaxies and Stellar Populations*, ed. B. M. Tinsley and R. B. Larson (New Haven: Yale University Observatory), p. 133.
Garmany, C. D., Conti, P. S. and Chiosi, C. 1982, *Ap. J.*, **263**, 777.
Hackwell, J. A., Grasdalen, G. L., and Gehrz, R. D. 1982, *Ap. J.*, **252**, 250.
Hayes, D. S. 1970, *Ap. J.*, **159**, 165.
Hayes, D. S., and Latham, D. W. 1975, *Ap. J.*, **197**, 593.
Hunter, D. A., Gallagher, J. S., and Rautenkranz, D. 1982, *Ap. J. Suppl.*, **49**, 53.
Israel, F. P. 1980, *Astr. Ap.*, **90**, 246.
Israel, F. P., Goss, W. M., and Allen, R. J. 1975, *Astr. Ap.*, **40**, 421.
Jensen, E. B., Talbot, R. J., and Dufour, R. J. 1981, *Ap. J.*, **243**, 716.
Kurucz, R. L. 1979, *Ap. J. Suppl.*, **40**, 1.
Mathis, J. S. 1970, *Ap. J.*, **159**, 263.
Mezger, P. G. 1978, in *Infrared Astronomy*, ed. G. Setti and G. G. Fazio (Dordrecht: Reidel), p. 1.
Miller, G. E., and Scalo, J. M. 1979, *Ap. J. Suppl.*, **41**, 513.
Osterbrock, D. E. 1974, *Astrophysics of Gaseous Nebulae* (San Francisco: W. H. Freeman).
Panagia, N. 1973, *A.J.*, **78**, 929.
Salpeter, E. E. 1955, *Ap. J.*, **121**, 161.
Sandage, A. and Tammann, G. A. 1974, *Ap. J.*, **194**, 559.
Scalo, J. M. 1978, in *Protostars and Planets*, ed. T. Gehrels (Tucson: University of Arizona), p. 265.
Shields, G. A., and Tinsley, B. M. 1976, *Ap. J.*, **203**, 66.
Smith, H. E. 1975, *Ap. J.*, **199**, 591.
Stone, R. P. S. 1977, *Ap. J.*, **218**, 767.
Stothers, R., and Chin, C. 1977, *Ap. J.*, **211**, 189.
———. 1979, *Ap. J.*, **233**, 267.
Strömgren, B. 1939, *Ap. J.*, **89**, 526.
Talbot, R. J. 1980, *Ap. J.*, **235**, 821.
Talent, D. L., and Dufour, R. J. 1979, *Ap. J.*, **233**, 888.
van der Kruit, P. C., Allen, R. J., and Rots, A. H. 1977, *Astr. Ap.*, **55**, 421.

K. DeGioia-Eastwood: Washburn Observatory, University of Wisconsin, 475 North Charter Street, Madison, WI 53706